

Quantifying the Cooling Effect of Tropical Cyclones on the Climate System

Liang Hu

UNSW

Elizabeth Ritchie (✉ liz.ritchie-tyo@monash.edu)

Monash University

J. Tyo

Monash University

Article

Keywords:

Posted Date: June 3rd, 2022

DOI: <https://doi.org/10.21203/rs.3.rs-1663318/v1>

License: © ⓘ This work is licensed under a Creative Commons Attribution 4.0 International License.

[Read Full License](#)

Version of Record: A version of this preprint was published at npj Climate and Atmospheric Science on July 24th, 2023. See the published version at <https://doi.org/10.1038/s41612-023-00433-z>.

Abstract

The net radiation due to 20 years of global tropical cyclones is calculated and the corresponding contribution to the earth energy balance is analyzed. Through their clouds, tropical cyclones are shown to increase the upwelling radiation at the top of the atmosphere compared with the clear sky condition. This provides an overall cooling effect on the climate system by increasing reflected shortwave (cooling) and decreasing emitted longwave (warming) radiation. The amount of cooling represents a considerable fraction of the excess warming energy in the climate system, but it is opposite in sign. While there are some tropical cyclones with net-warming effect, the majority are net cooling and these tend to represent both more intense and earlier-season systems. Current understanding predicts an increase in the proportion of intense tropical cyclones due to a warming climate, so this cooling effect serves as potential negative feedback on the warming climate system.

1. Introduction

The primary driver of the Earth's climate system is the distribution of net downward radiation at the top of the atmosphere (TOA) owing principally to the Sun–Earth geometry. Clouds are an essential component of the re-distribution of this solar energy in the climate system through their effect on shortwave (SW) and longwave (LW) radiative fluxes, as well as their contribution to energy re-distribution through phase changes of water. Thus, they are an important component of the radiation budget and earth energy balance.

The interactions among clouds and other components of the Earth climate system are quite complex, and they are an area of active investigation (1-3). A large amount of the incoming solar energy is directly reflected at the TOA by clouds, and this effect dominates in the SW radiation regime (wavelengths less than 3 μm). In the LW regime (wavelengths longer than 3 μm), thermal processes dominate. Thermal radiative energy is released by all elements of the earth's surface with the spectral peak in the LW regime dependent on the apparent temperature of the emitting components. Since clouds generally reduce LW penetration (4), their presence limits the amount of LW radiation released from the surface of the earth (5-7) that can escape into space. The cloud then re-emits at a colder apparent temperature that depends on cloud height, reducing the net upwelling LW radiative flux. Of the two mechanisms, SW reflectance increases the total upwelling radiation and acts as a cooling effect on the earth energy balance, while LW attenuation reduces the upwelling radiation and acts as a warming effect.

The overall contribution of clouds to the radiation budget is complicated and depends on the specifics of the Earth-ocean-atmosphere system. With a globally averaged cloud-radiative effect of 20 W m^{-2} , clouds act to strongly cool the planet (8) [1]. However, as the climate warms, clouds and their radiative effects are expected to increase, providing a feedback signal that is most likely negative (i.e., a cooling effect in a warming planet), but highly uncertain (8-10). Improving our understanding of the role of clouds in climate is crucial to understanding the effects of global warming.

In recent decades, a great deal has been learned about clouds and their radiation contribution to the earth energy balance (11, 12). However, the specific impact of clouds due to organised mesoscale convective systems such as tropical cyclones on the earth energy balance is relatively unknown. Most tropical cyclone studies examine intensity, track and precipitation, but little is known about their radiation contribution to the earth energy balance. There are three reasons for the lack of research in this area. First, compared with tropical cyclone characteristics such as intensity and precipitation, their radiation does not cause direct major damage and is not of immediate concern. Second, as tropical cyclones are surrounded by other cloud systems with which they have complicated interactions, it is difficult to decide the boundary of the tropical cyclone and non-tropical cyclone cloudy regions. Third, many tropical cyclones need to be analyzed over a long period of time in order to draw conclusions about their radiation impact on the earth energy balance.

The question of how tropical cyclones may change in a warmer climate has been discussed broadly. A theoretical study showed that a significant increase in tropical cyclone intensity will likely occur in a warming climate (13). Webster, et al., examined the number of tropical cyclones and cyclone days as well as tropical cyclone intensity over 35 years in an environment of increasing sea surface temperature. They found that there has been a large increase in the number and proportion of hurricanes reaching categories 4 and 5, while the overall number of cyclones and cyclone days has decreased (14). However, their study was limited by inconsistencies in the global tropical cyclone best track archives that underpin their study. Global model studies have documented the potential effects of climate change on tropical cyclones (15-19). While there is wide variation in the results of these studies, the consensus is for a tendency toward decreasing frequency, increasing proportion of intense, and increasing precipitation of tropical cyclones as the climate warms (19-21). However, there is currently little information on how the structure, size, convective activity, or seasonal activity of tropical cyclones will change. One study did find a positive feedback mechanism between tropical cyclones and climate warming through the strengthening of the Kuroshio current over the western Pacific Ocean (22). Although there has been a significant number of research studies on the variation of tropical cyclone activity due to climate change, there are few studies about the impact of a warming climate on tropical cyclone cloud net radiation or on the feedback that tropical cyclone cloud net radiation provides to the climate system.

With the advancement of remote sensing technology, satellite images have been used extensively to assess tropical cyclone intensity (23-27), tropical cyclone genesis (28), tropical cyclone location and tracking (23-25, 29), wind structure (30-32), and precipitation (33-35). In addition, there have been some attempts to isolate the tropical cyclone in satellite images using segmentation algorithms mostly for tracking purposes (30, 36).

We recently presented a semi-automated remote sensing framework that successfully segments tropical cyclone clouds in satellite images (37). We then used the segmented images to compute the global contribution of tropical cyclone clouds to the upwelling radiation during 2016 and found that tropical cyclones were responsible for a net increase in upwelling radiation compared to the clear-sky condition that is significant compared with the surplus energy in the earth energy balance (40.5 TW upwelling

(cooling) in 2016 due to tropical cyclones, compared with the ~ 300 TW energy surplus (warming) in the earth energy balance (38)). Although the overall impact of tropical cyclones on the earth energy balance in this single year of data is net-cooling, there is a distribution of results for individual storms that range from slightly warming to significantly cooling (37). To date, there is no understanding of what drives this distribution. In addition, while we demonstrated that tropical cyclones may produce an increase in upwelling radiation that is large enough to have an impact on the global earth energy balance, the original study did not consider a long enough data set to robustly quantify the overall result, consider whether there are regional differences, or consider how changes in tropical cyclone activity might affect the earth energy balance. In this paper, we expand the data set to include all tropical cyclones globally from 2001 to 2020 to verify the conclusions in (37) over a longer-term period. In addition, we explore the interannual, regional, and diurnal variation of the signature in order to understand how tropical cyclone cloud activity impacts the earth energy balance. Finally, we develop an understanding of the types, physical characteristics, seasonality, and locations of tropical cyclones that produce net positive (cooling) or negative (warming) totals to the earth energy balance and discuss the implications of these findings for a warming climate.

[1] Throughout this paper we use the convention that *upwelling* radiation is *positive*. An increase in upwelling radiation represents a cooling effect.

2. Results

Two computational methods have been used to analyse the radiative contributions of tropical cyclone clouds, which are described in detail in the Methods section below. The first is a mask that only includes the cold clouds representing the most intense convection of the storm (cloud mask – hereafter C_{mask}). The second includes all pixels that fall within a circle that circumscribes the cloud mask (R_{max}). The two calculation methods result in a quite large difference in the final net radiation result. The C_{mask} calculation considers cloudy pixels colder than a threshold brightness temperature and so excludes both warm cloud pixels and the “moats” of clear sky between convective bands that are inherently part of the tropical cyclone structure. The R_{max} calculation includes the additional warmer cloud and surface pixels that are excluded from the C_{mask} calculation. These low-level warm pixels reflect SW radiation and also radiate more strongly in the infrared spectrum than high cold cloud pixels and contribute additional net positive upwelling particularly during the nighttime when SW reflectance is zero. In general, the C_{mask} calculation provides a lower bound on the net radiation due to the tropical cyclone and the R_{max} provides an upper bound estimate, which is 3–4 times higher than the C_{mask} estimate for the total radiation contribution to the earth energy balance due to tropical cyclones. Both bounds are important because of the need to understand how much tropical cyclones contribute to the radiation budget and how changes in tropical cyclone activity in the future may impact that budget and the overarching conclusions of the paper are not affected by which calculation we choose to use. To present the results here, quantitative results are presented and discussed only for the more conservative C_{mask} unless there are large differences that require discussion. The equivalent numbers for R_{max} are presented in the text in

parentheses next to the C_{mask} results and figures for R_{max} are also provided in each figure panel for comparison.

2.1 Global Annual Upwelling Radiation from Tropical Cyclones

The annual net radiation and frequency distribution of 2038 global tropical cyclones are shown in Fig. 1. The annual tropical cyclone net radiation is positive throughout the 20-year period, amounting to an annualized average flux of 56.1 TW (223.3 TW) (Fig. 1a). Regardless of the calculation method, the tropical cyclone net contribution represents a cooling effect on the climate system. When compared with the estimated 300 TW per year of total excess energy in the climate system due to greenhouse gases (38), then the tropical cyclone upwelling contribution represents an important cooling effect on the climate system of 18% (74%) of the total excess energy. In an environment of increasing tropical cyclone activity, this would represent *negative* feedback, which serves to stabilize the overall climate system.

The tropical cyclone net radiation varies annually over the 20-year period. It is highly correlated with the number of tropical cyclone days (0.79 (0.81)) and less so with the number of tropical cyclones (0.45 (0.46)) that form each year. There is a period of higher tropical cyclone-contributed net radiation during 2002–2005, a period of lower tropical cyclone net radiation contribution during 2006–2010, and considerable fluctuation between 2011 through 2020 (Fig. 1). In addition, there is a strong seasonal pattern that follows the tropical cyclone seasonal cycle with a maximum in tropical cyclone-related net radiation in August (northern hemisphere) and January (southern hemisphere) (Fig. 1b). Minimum tropical cyclone-related net radiation occurs in November and April, which are the transition months between tropical cyclone seasons in the northern and southern hemispheres. In both hemispheres, 95% (88%) of the net tropical cyclone radiation is contributed between the spring and autumn equinoxes (Figs. 1b, 1c) also consistent with the relatively higher (70%) tropical cyclone activity during that period. The annual and seasonal variation suggests that the tropical cyclone net radiation contributes more to the earth energy balance in some years, and it plays a larger role during the northern hemisphere peak tropical cyclone season.

The annual proportion of tropical cyclones, tropical cyclone days and net radiation by tropical cyclone basin for the Western North Pacific (WP), Eastern North Pacific (EP), North Atlantic (NA), North (NI) and South (SI) Indian, and South Pacific (SP) Oceans is shown in Fig. 2. The WP has by far the largest annual average tropical cyclone numbers (Fig. 2a) and tropical cyclone days (Fig. 2b) of all the six global tropical cyclone basins. This coincides with it producing the highest annual average net radiation contribution to the earth energy balance (Figs. 2c, 2d) although the proportion of net radiation produced by the WP is higher relative to the proportion of tropical cyclone activity (measured by number of tropical cyclone days or total number of tropical cyclones) in that basin (Fig. 2). This is also true for the SP basin. The NI produces the lowest annual average tropical cyclone net radiation contribution. The net radiation produced by tropical cyclones in both the NI and NA is proportionally lower than the corresponding tropical cyclone activity (Fig. 2).

The daily cycle of net radiation averaged over all tropical cyclones globally exhibits a distinct diurnal cycle (Fig. 3) with a tendency for positive net radiation during the day when direct reflection of the incoming SW radiation is maximised and negative net radiation at night when only LW emission contributes to the net upwelling radiation. In addition, the tropical cyclone net radiation during the day varies with the solar SW intensity, but it tends to be relatively constant at night. Overall, the magnitude of the positive net integrated radiation in the daytime is larger than that of the negative net integrated radiation at night, due in part to the fact that tropical cyclones primarily occur before the local autumnal equinox (Fig. 1c) when incoming SW solar radiation is maximised. The average net tropical cyclone radiation over one 24-hour period is approximately + 0.084 TW (+ 0.335 TW), indicating the daily cooling effect of tropical cyclone clouds on the earth relative to the clear sky condition.

2.2 Individual tropical cyclone contribution and distribution

While the overall contribution of tropical cyclones to the earth energy budget is positive, some tropical cyclones contribute positive net radiation while others contribute negative net radiation over their lifetime, and some contribute higher amounts than others. Figure 4 shows the frequency distribution by magnitude and sign of net radiation for all 2038 tropical cyclones over their lifetimes. Most tropical cyclones produce net radiation between - 1 and 1 TW over their lifetime (Fig. 4a). Twenty-one percent of tropical cyclones produce a net positive radiation > 1 TW and only a very small fraction (0.3%) produce net negative radiation < -1 TW. The R_{max} calculation produces a larger spread of values for each tropical cyclone than the C_{mask} calculation (Fig. 4b), as well as a larger proportion of higher magnitude positive net radiation tropical cyclones, which contributes to the larger overall net radiation produced using this method. Tropical cyclones that produce net positive radiation over their lifetime also exist for, on average, 1.2 days longer than those that produce net negative radiation, which also contributes to their larger overall net radiation contribution (Figs. 4, S2a). Overall, the vast majority of tropical cyclones (83% (87%)) produce a positive net radiation (referred to as PNR tropical cyclones hereafter) with an associated *cooling effect*, while approximately 17% (13%) of the tropical cyclones have negative net radiation (NNR tropical cyclones hereafter) with a *warming effect* (Table 1) over their lifetimes. With the exception of the NI basin, the distribution of NNR and PNR tropical cyclones (Fig. S1) and percentage of PNR tropical cyclones is remarkably similar across basins, ranging from 81% (85%) in the SI to 88% (95%) in the EP (Table 1). The percentage of PNR tropical cyclones in the NI basin is much lower (65% (57%)), the lifespans more even (Fig. S2), and the distribution is much more tightly constrained around 0 TW (Fig. S1d, S1j) with a higher proportion of NNR TCs leading to the lowest basin-specific accumulated tropical cyclone net radiation of all six ocean basins (Fig. 2).

Table 1

The total number* of PNR and NNR tropical cyclones globally and by ocean basin calculated using the C_{mask} and R_{max} calculations.

		WP	EP	NA	NI	SP	SI	Total
PNR tropical cyclones	C_{mask}	502 (85%)	385 (88%)	271 (82%)	103 (65%)	169 (86%)	277 (81%)	1707 (83%)
	R_{max}	537 (91%)	413 (95%)	304 (92%)	90 (57%)	169 (86%)	288 (85%)	1801 (88%)
NNR tropical cyclones	C_{mask}	87 (15%)	52 (12%)	61 (18%)	55 (35%)	27 (14%)	64 (19%)	346 (17%)
	R_{max}	52 (9%)	24 (6%)	28 (8%)	68 (43%)	27 (14%)	53 (16%)	252 (12%)
*Percent of basin total is provided in brackets.								

To better understand why a tropical cyclone is NNR or PNR over its lifetime, factors contributing to the diurnal cycle of the cloud net radiation signal for PNR and NNR tropical cyclones are compared in Fig. 5. Figure 5a indicates that both PNR and NNR tropical cyclones have more clouds at night (1800 – 0600 LST) than during the daytime (0600–1800 LST). In addition, the net radiation intensity and overall net radiation due to tropical cyclones is negative for all tropical cyclones and of similar magnitude at nighttime regardless of whether the tropical cyclone is PNR or NNR (Figs. 5b, 5c), indicating that the cloud top temperatures associated with the two types of tropical cyclones are similar producing similar LW upwelling. Thus, it is the daytime differences that determine whether the tropical cyclone is PNR or NNR. During the day, the main factors that affect the radiation are the cloud fraction, the sun elevation, and the length of day. PNR tropical cyclones have a larger amount of clouds during the day than NNR tropical cyclones (Fig. 5a), which produces more reflected SW radiation. In addition, the net radiation intensity is higher for PNR compared with NNR tropical cyclone clouds during the day, and PNR tropical cyclones produce positive net radiation intensity for a longer period during the day (Fig. 5b). This is because in both the northern and southern hemispheres, the majority of PNR tropical cyclones occur during the summer whereas the peak NNR tropical cyclones lag by 2–3 months and occur predominantly after the autumnal equinox (Fig. S3). Thus, the solar elevation angle and length of day is higher for PNR tropical cyclones compared with NNR tropical cyclones resulting in a higher SW reflectance and positive net radiation for PNR tropical cyclones. The only exception to this is in the NI basin where there is a double peak in tropical cyclone activity, one in May and a larger peak in October/November with a lull in the summer during the peak of the monsoon. In this basin there is a higher percentage of NNR activity compared with the other basins (Fig. S3, Table 1) because of the much higher proportion of late season tropical cyclones that form when the sun angle is relatively low. Combining the cloud amount (Fig. 5a) with the net radiation intensity (Fig. 5b) gives the diurnal cycle of overall net radiation (Fig. 5c), which

shows that across the entire 24-hour period, PNR tropical cyclones generally produce more positive net radiation than NNR tropical cyclones during the daytime (Fig. 5c), which overwhelms the negative net radiation produced during the night-time.

Finally, the frequency of tropical cyclone net daily radiation plotted against daily peak cloud shield size and daily peak intensity is provided in Fig. 6. Here, size is calculated as the equivalent radius of a circle with the same number of pixels as the C_{mask} . On average, there are more instances of daily net positive radiation due to tropical cyclones compared with daily net negative radiation, and the magnitude increases more with size for positive radiation cases than for negative radiation cases (Fig. 6a). In particular, in the WP, EP, SI, and SP, there is a higher tendency for higher net positive radiation that increases with cloud size (Fig. S4a). In contrast, the NI clearly exhibits a tendency for higher frequency of daily *net negative radiation*, and this also increases with cloud size. Furthermore, there is a higher tendency for tropical cyclones that produce daily net negative radiation to be lower in intensity (< 45 kts) (Figs. 6b, S4b, S5), whereas tropical cyclones that produce a daily net positive radiation are skewed to higher intensities (> 45 kts) (Figs. 6b, S4b, S5). Finally, the frequency and magnitude of daily positive net radiation is higher than net negative radiation across all intensities with the exception of the NI (Fig. 6, S4b).

In summary, most tropical cyclones produce net positive radiation both on a daily basis and over their lifetimes, which leads to an overall positive net radiation (cooling) signal globally due to tropical cyclones. The daily and lifetime tropical cyclone contribution to net radiation is positive when the SW reflectance during the day is higher than the 24-hour LW emission. Factors that contribute to net positive radiation include the size of the tropical cyclone cloud shield, the length of day, and the sun elevation angle, which is highest between the spring and autumn equinoxes and coincides with the majority of tropical cyclone activity globally.

2.3 Spatial distribution of net radiation due to tropical cyclones

The spatial distribution of tropical cyclone frequency density and tropical cyclone net radiation per year are shown in Fig. 7. The general pattern of tropical cyclone net radiation matches the spatial distribution of tropical cyclone cloud frequency (Figs. 7a, 7c, 7d). The majority of the tropical cyclone affected areas have positive net radiation (blue shading - cooling effect) both for tropical cyclones (Figs. 7c and 7d) and for all of the clouds (Fig. 7b) over the year. There are two maxima (> 0.016 TW per pixel annualized), one over the northwest and one over the northeast Pacific regions, which correspond to peaks in the tropical cyclone frequency density. There are some regions of net negative tropical cyclone radiation near the equator in the SI, SP, and WP, as well as in the Arabian Sea and the mid-Atlantic (brown shading - warming effect). Over the arid and semi-arid Australian continent, Indian subcontinent, and the southwest portion of North America, both the tropical cyclone and all cloud contributions to the net radiation are negative. In these regions the relative humidity in the daytime is much lower than that during the night-time, thus more tropical cyclone clouds form at night over these regions. These are also regions where tropical

cyclones are dissipating after making landfall and their clouds are relatively warmer, although still colder than the ground. Overall, the magnitude of the LW radiation contribution for tropical cyclones in these semi-arid land regions is greater than that of the SW radiation, contributing to an overall negative net radiation (warming effect).

The tropical cyclone net radiation contribution (Figs. 7e and 7f) to all clouds net radiation shows that the tropical cyclone net radiation accounts for a large proportion of the “all cloud” radiation. There are small regions in the WP main development region, off the Northwest Shelf of Australia, the Arabian Sea and portions of the Bay of Bengal where the contribution due to tropical cyclones is opposite in sign to the “all cloud” contribution. However, the contribution over the WP, EP and northern Australia is more than 20% of the “all cloud” contribution, which indicates that the tropical cyclone net radiation can have significant impact on the regional contribution to the earth energy balance (39, 40). Notably, these are in open-ocean regions that, in the absence of cloud, would be responsible for significant absorption of downwelling solar flux.

3. Discussion

The net radiation for 2038 tropical cyclones from 2001 to 2020 is calculated using a semi-automated cloud segmentation algorithm. Two different calculations are performed providing an upper- and lower bound for net radiation due to tropical cyclones. The C_{mask} calculation provides a lower estimate of total emitted radiation because it excludes warmer clouds and earth surface within the dynamic boundaries of the storm that are below the brightness threshold cut-off within the tropical cyclone circulation. These relatively warm areas contribute higher emitted upwelling radiation compared to colder clouds and so contribute to a higher estimate of emitted net radiation when included in the R_{max} calculation. However, regardless of the calculation method used, the overarching conclusion is the same – *that tropical cyclones are a net positive contribution to the upwelling radiation and therefore are a net negative (cooling) effect on the earth energy balance.* This has important implications because:

1. The contribution by tropical cyclones to the earth energy balance over the past 20 years is of similar magnitude, and opposite sign to the excess energy in the climate system. That is, tropical cyclones are a large contributing factor to offsetting global warming. Changes in this net contribution due to future tropical cyclone changes will be important;
2. Current projection consensus is for a decrease in tropical cyclone numbers but increase in frequency of the higher intensity tropical cyclones. As more intense tropical cyclone days are likely to be PNR, a higher proportion of more intense tropical cyclones may lead to a higher cooling contribution.
3. The net radiation contribution by tropical cyclones is more dependent on the number of tropical cyclone days rather than the number of tropical cyclones. Current projections do not provide information about the future number of tropical cyclone days.
4. The net radiation contribution by tropical cyclones is dependent on when they form in the season – late-season tropical cyclones are more likely to be NNR, and the tropical cyclone cloud size – higher

cloud amounts are more likely to be high PNR, and on the longevity of the tropical cyclone. Current projections do not provide information about future trends.

The data presented above allow us to draw several conclusions about the mechanisms for the significant net cooling contribution that tropical cyclones make to the earth energy balance. Most importantly, the net radiation of any particular storm is tightly linked to the diurnal balance between daytime reflected radiation and the 24-hour emitted infrared radiation. During the day, the large cloud cover produced by tropical cyclones creates a significant increase in the upwelling radiation due to reflected SW radiation at the top of the atmosphere. At night there is no downwelling radiation to reflect, so the upwelling radiation is all LW emitted radiation. Since tropical cyclone clouds are generally much colder than the surface, this leads to a decrease in upwelling radiation at night. Whether any particular storm is PNR or NNR depends on this balance. However, since both NNR and PNR tropical cyclones emit similar amounts of radiation at night, it is differences in the daytime radiation that lead to a tropical cyclone being PNR or NNR. The primary differences between PNR and NNR tropical cyclones are that during the day PNR tropical cyclones have a higher cloud amount, they produce higher peak net radiation intensity, and produce net positive radiation for a longer period compared with NNR tropical cyclones. For NNR tropical cyclones, the daytime SW reflectance is lower than the overall LW reflectance resulting in net negative radiation. A large part of the reason why the PNR tropical cyclone signal is dominated by the SW effect is that they tend to occur between the local vernal and autumnal equinoxes so that the longer day and higher sun angle results in higher SW reflectance. Because the majority of tropical cyclones occur during these months the majority of tropical cyclones globally (~ 83%) are PNR.

Second, the distribution of PNR storms is skewed to higher intensities and they have longer lifespans, while the reverse is true of NNR storms. PNR tropical cyclones tend to occur earlier in the season with a peak in PNR activity occurring 2–3 months ahead of the peak in NNR tropical cyclones in all basins except the NI. This is when sea-surface temperatures are warmest, and the environment is most supportive of tropical cyclones.

Third, the geographic distribution of radiation attributable to tropical cyclones closely follows the spatial distribution of tropical cyclone frequency. However, what may be more important is how much of the radiation in each region is due to tropical cyclones and regional differences that lead rise to a higher proportion of NNR versus PNR tropical cyclones in some regions. In the NI basin tropical cyclones form either very early in the season before the summer solstice, or late in the season (peak activity) well after the autumnal equinox and thus produce a higher percentage of NNR tropical cyclones resulting in overall a mixture of weak net negative and positive upwelling radiation. In the EP, WP and NA basins, tropical cyclones account for a very large percentage (> 20%) of the total net radiation from all clouds, even though these regions generally (with the exception of the EP) do not contribute particularly high percentages of the total annual net radiation. This latter point suggests that tropical cyclones are responsible for generating a significant portion of the cloud cover over what would otherwise be very low albedo open ocean.

There are a few regions of the earth where the total radiation contribution from tropical cyclones is net negative (warming). These include the Australian continent, SW deserts of N. America, and the Arabian Peninsula, which are arid generally high-albedo land regions. Landfalling tropical cyclones bring more disorganised, warmer cloud cover that does not increase the reflected SW over these regions as much as over ocean regions, but causes a significant reduction in emitted LW. This results in a net negative (warming) radiation contribution by tropical cyclones in these regions. There are also two anomalous regions in the mid-Pacific Ocean straddling the equator and one in the South Indian Ocean that have net negative radiation contribution. The causes of these anomalies are still under investigation.

There are three caveats to the results presented in this study. First, we have compared the radiation from tropical cyclones to the clear-sky condition, but it is not clear that is exactly the right comparison. A more directly relevant comparison would be with the hypothetical situation where the tropical cyclone was not present, but other clouds such as mesoscale convective systems were still allowed to exist. Second, in order to bound the true effect of the tropical cyclone, we have considered two extreme cases of pixel masks. The first only considers specific pixels identified as cold tropical cyclone clouds. The second includes all pixels surrounding the tropical cyclone up to a radius that circumscribes the cloud pixel mask. The overall trends are independent of the choice of mask, but the absolute quantity of radiation differs by a factor of 3–4. Understanding the proper baseline against which to make the comparison is an ongoing topic of research. Third, the time series of each tropical cyclone in the dataset is truncated as described in the methods section, to ensure the tropical cyclone net radiation is calculated in consistent 24-hour periods reflecting equal parts daytime and night-time periods. This results in an average reduction in the considered lifetime of 6–7% across all tropical cyclones, and reduces the net radiation attributed to tropical cyclones.

Previous studies indicate that there will be a higher proportion of strong tropical cyclones in a future warming climate (42, 43). If that occurs, then this study suggests there will be more positive net radiation with a corresponding cooling effect produced by the increasingly stronger tropical cyclones. In other words, this study suggests that the increasing proportion of strong tropical cyclones predicted to occur as the Earth warms will likely act as a negative (cooling) feedback, which may contribute to maintaining overall balance in the system.

4. Materials And Methods

4.1 Data

To quantify the upwelling radiation due to tropical cyclones, three sources of data from the National Oceanic and Atmospheric Administration (NOAA) and the National Aeronautics and Space Administration (NASA) are used (Table S1). The NOAA International Best Track Archive for Climate Stewardship (IBTrACS) tropical cyclone best-track dataset (44) provides all tropical cyclone locations over all tropical cyclone basins. The NCEP/CPC Global Merged IR Brightness Temperature Dataset (GPM_MERGIR) (45) is used to segment the tropical cyclone clouds, and the Clouds and Earth's Radiant Energy System (CERES)

TOA dataset (46) is used to calculate the radiation contribution by tropical cyclones. The period of study is 2001–2020.

4.2 Tropical Cyclone cloud labelling

The hourly tropical cyclone center positions from the best-track data were linearly interpolated to match the half-hourly temporal resolution of the brightness temperature data, enabling the segmentation algorithm to be performed at high frequency. Full details of the segmentation algorithm can be found in (37). The tropical cyclone cloud segmentation task is accomplished by a semi-automated algorithm which takes a time series of brightness temperature images of tropical cyclones and uses image processing techniques to segment each image and label all tropical cyclone cloud pixels. An example of labels determined by the segmentation algorithm is shown in Fig. S6 for TC Newton in September 2016 in the EP basin, showing results at 4 instances through the tropical cyclone life. This result illustrates the ability of the algorithm to successfully segment the cloud coverage of TC Newton and capture changes in the tropical cyclone shape across instances. Full results for all tropical cyclones globally in 2016 are available in the IEEE Dataport that demonstrate the robustness of the method (<https://iee-dataport.org/open-access/2016-tropical-cyclone-cloud-segmentation#files>).

4.3 Description of cloud masks

In this study, two cloud masks are used to calculate the tropical cyclone radiation. The first is based on the radiation due only to the cloud pixels identified by the segmentation algorithm described by Nguyen, *et al.*, (37, C_{mask}), and the second considers the radiation contribution from a circular mask centered on the tropical cyclone with a radius that captures all cloudy pixels identified by the algorithm, but also considers the pixels within the circle that aren't labelled in the cloud mask (R_{max}). The R_{max} calculation provides a much higher net radiation contribution compared to the C_{mask} calculation because the moat regions made up of low-level clouds and earth surface between tropical cyclone rainbands, which are generated due to the tropical cyclone dynamics, are included in the radiation calculation. However, the perfectly circular region considered almost certainly includes regions that are not part of the cyclone dynamics. In contrast, the C_{mask} calculation has a cold brightness temperature threshold above which pixels are not included in the calculation, and so these warmer pixels in the moat regions are not counted in the C_{mask} . Thus, the R_{max} calculation is always 3 to 4 times higher than the C_{mask} calculation. Both masks are indicated on the images in Fig. S6. The main body of the paper focuses on the results from the C_{mask} and the R_{max} results are included in parentheses and in the figures. The results from both masks are included in this paper because they produce approximate upper and lower bounds to the contribution from tropical cyclones, as the areas within the storm that do not have cold enough clouds to be picked up by the cloud label algorithm are almost certainly important.

4.4 Calculation of Net Radiation

The radiation contribution of each pixel within the masks is calculated by combining the segmentation results with the CERES radiation dataset via a coordinate-matching scheme that is necessary due to the

difference in spatial resolution of the two datasets (37). Finally, the amount of all tropical cyclone net radiation is calculated by subtracting the “clear-sky” radiation product provided in the CERES data set (46) from the total upwelling radiation. When the net upwelling radiation with the tropical cyclone present is *higher* than the clear-sky radiation, the pixel has a *positive* contribution that is net *cooling*. Likewise, when the net upwelling radiation is *negative*, that pixel has a net *warming* effect on the earth energy balance.

4.5 Consistent period for radiation calculation

Tropical cyclone net radiation depends on the difference between SW radiation and LW radiation, and since SW reflectance occurs only during the daytime, the balance of the tropical cyclone cloud distribution during the day and night is important. However, the lifetime of a tropical cyclone as defined in the IBTrACS best track database is almost never an integer number of 24-hour periods. Furthermore, as the tropical cyclone traverses the basin, local solar time (LST) is more important than 24-hour periods in describing the impact of the tropical cyclone on the earth energy balance because of its effect on the SW reflectance. Thus, the time of genesis and end-of-life in LST has an impact on tropical cyclone energy statistics. Table S2 quantifies this effect by examining the average contribution of the extra fraction of a day removed to round the tropical cyclone lifetime down to a full integer day. PNR tropical cyclones lose on average 0.3 days mostly during in the daytime, which is 4.7% of the time record, but 8.4% in net radiation to the entire tropical cyclone. NNR tropical cyclones lose on average 0.4 days at night, which is 6.7% in time but 25.9% in net negative radiation, which is lost to the entire tropical cyclone life span. However, Table S2 demonstrates that PNR tropical cyclones are, on average, net positive both for the integer number of full-days and the extra time, while NNR tropical cyclones are, on average, net negative for both intervals. Thus, although both types of tropical cyclones radiation contribution through the truncation to whole day periods the loss is of the same sign as the overall contribution by that tropical cyclone.

Even though Table S2 shows that truncating each tropical cyclone time series to integer LST days results in a loss of time and net radiation for both NNR and PNR tropical cyclones the integer LST days [integer × (00–24 LST)] are used in calculating the tropical cyclone net radiation in this study to avoid the effects of a subjective determination of the tropical cyclone begin and end time. Testing demonstrated that there is no change to the overall conclusion of this study if the entire tropical cyclone lifespan data are used. However, by constraining the data to integer LST days we ensure we do not include additional points in either the daytime or the night-time that represent an arbitrary “start” and “end” determination that would bias our results to net positive or net negative impact on the earth energy balance.

Data and materials availability

Data underlying the study will be made available through UNSWorks. DOI will be made available prior to publication.

Declarations

Acknowledgments: This research is supported by an Australian Research Council Discovery Project grant DP210103203.

Author contributions:

L.H. performed the research, contributed to analyzing the results, and wrote the first draft of the manuscript.

E.A.R contributed to conceptualizing the science problem, designing the methodology, analyzing results, providing supervision to L.H., and revising the manuscript.

J.S.T. contributed to conceptualizing the science problem, designing the methodology, analyzing results, providing supervision to L.H., and revising the manuscript.

Competing interests: The authors declare no competing interests.

References

1. A. Arking, The radiative effects of clouds and their impact on climate. *Bulletin of the American Meteorological Society*. **72**, 795–814 (1991).
2. P. V. Hobbs, *Aerosol-cloud-climate interactions*. (Academic Press. San Diego, California, 1993)
3. G. L. Stephens, Cloud feedbacks in the climate system: A critical review. *Journal of climate*. **18**, 237–273 (2005).
4. J. T. Kiehl, K. E. Trenberth, Earth's annual global mean energy budget. *Bulletin of the American meteorological society*. **78**, 197–208 (1997).
5. X. Ge, Y. Ma, S. Zhou, T. Li, Impacts of the diurnal cycle of radiation on tropical cyclone intensification and structure. *Advances in Atmospheric Sciences*. **31**, 1377–1385 (2014).
6. C. B. Michael, M. T. Bell, B. R. Brown, Impacts of radiation and upper-tropospheric temperatures on tropical cyclone structure and intensity. *J. Atmospheric Sci*. **76**, 135–153 (2019).
7. J. H. Ruppert, A. A. Wing, X. Tang, E. L. Duran, The critical role of cloud-infrared radiation feedback in tropical cyclone development. *Proc. Nat. Acad. Sci. USA*, **117**, 27884–27892 (2020).
8. O. Boucher, D. Randall, “Clouds and aerosols” in *Climate change 2013: the physical science basis. Contribution of Working Group I to the Fifth Assessment Report of the Intergovernmental Panel on Climate Change* (IPCC, Cambridge University Press, Cambridge, United Kingdom and New York, NY, 2013).
9. B. J. Soden, I. M. Held, R. Colman, K. M. Shell, J. T. Kiehl, C. A. Shields, Quantifying climate feedbacks using radiative kernels. *Journal of Climate*. **21**, 3504–3520 (2008).
10. J. Vial, J. L. Dufresne, S. Bony, On the interpretation of inter-model spread in CMIP5 climate sensitivity estimates. *Climate Dynamics*. **41**, 3339–3362 (2013).

11. A. E. Dessler, Cloud variations and the Earth's energy budget. *Geophysical Research Letters*. **38**, L19701 (2011).
12. A. Otto, F. Otto, O. Boucher, J. Church, G. Hegerl, P. M. Forster, N. P. Gillett, J. Gregory, G. C. Johnson, R. Knutti, N. Lewis, U. Lohmann, J. Marotzke, G. Myhre, D. Shindell, B. Stevens, M. R. Allen, Energy budget constraints on climate response. *Nature Geosci.* **6**, 415–416 (2013).
13. K. A. Emanuel, The dependence of hurricane intensity on climate. *Nature*. **326**, 483–485 (1987).
14. P. J. Webster, G. J. Holland, J. A. Curry, H. R. Chang, Changes in tropical cyclone number, duration, and intensity in a warming environment. *Science*. **309**, 1844–1846 (2005).
15. L. Bengtsson, M. Botzet, M. Esch, Will greenhouse gas-induced warming over the next 50 years lead to higher frequency and greater intensity of hurricanes? *Tellus A*. **48**, 57–73 (1996).
16. M. Sugi, A. Noda, N. Sato, Influence of the global warming on tropical cyclone climatology: An experiment with the JMA global model. *Journal of the Meteorological Society of Japan*. Ser. II. **80**, 249–272 (2002).
17. K. Oouchi, J. Yoshimura, H. Yoshimura, R. Mizuta, S. Kusunoki, A. Noda, Tropical cyclone climatology in a global-warming climate as simulated in a 20 km-mesh global atmospheric model: Frequency and wind intensity analyses. *Journal of the Meteorological Society of Japan*. Ser. II. **84**, 259–276 (2006).
18. J. Yoshimura, M. Sugi, A. Noda, Influence of greenhouse warming on tropical cyclone frequency. *Journal of the Meteorological Society of Japan*. Ser. II. **84**, 405–428 (2006).
19. L. Bengtsson, M. Botzet, M. Esch, Hurricane-type vortices in a general circulation model. *Tellus A*. **47**, 175–196 (1995).
20. J. H. Christensen, K. K. Kanikicharla, “Climate phenomena and their relevance for future regional climate change” in *Climate change 2013: the physical science basis. Contribution of Working Group I to the Fifth Assessment Report of the Intergovernmental Panel on Climate Change* (IPCC, Cambridge University Press, Cambridge, United Kingdom and New York, NY, 2013).
21. S. I. Seneviratne, X. Zhang, M. Adnan, W. Badi, C. Dereczynski, A. Di Luca, S. Ghosh, I. Iskandar, J. Kossin, S. Lewis, F. Otto, I. Pinto, M. Satoh, S.M. Vicente-Serrano, M. Wehner, B. Zhou, “Weather and climate extreme events in a changing climate” in *Climate change 2021: the physical science basis. Contribution of Working Group I to the Sixth Assessment Report of the Intergovernmental Panel on Climate Change* (IPCC, Cambridge University Press, Cambridge, United Kingdom and New York, NY, 2021).
22. Y. Zhang, Z. Zhang, D. Chen, B. Qiu, W. Wang, Strengthening of the Kuroshio current by intensifying tropical cyclones. *Science*, *368*(6494), 988–993 (2020).
23. V. F. Dvorak, Tropical cyclone intensity analysis and forecasting from satellite imagery. *Monthly Weather Review*. **103**, 420–430 (1975).
24. C. S. Velden, T. L. Olander, R. M. Zehr, Development of an objective scheme to estimate tropical cyclone intensity from digital geostationary satellite infrared imagery. *Weather Forecasting*. **13**, 172–186 (1998).

25. M. F. Pineros, E. A. Ritchie, J. S. Tyo, Objective measures of tropical cyclone structure and intensity change from remotely sensed infrared image data. *IEEE Trans. Geosci. Remote Sens.* **46**, 11, 3574–3580 (2008).
26. T. L. Olander, C. S. Velden, The advanced Dvorak technique: Continued development of an objective scheme to estimate tropical cyclone intensity using geostationary infrared satellite imagery. *Weather Forecasting.* **22**, 287–298 (2007).
27. L. Hu, E. A. Ritchie, J. S. Tyo, Short-term tropical cyclone intensity forecasting from satellite imagery based on the deviation angle variance technique. *Weather and Forecasting.* **35**, 285–298 (2020).
28. M. F. Pineros, E. A. Ritchie, J. S. Tyo, Detecting tropical cyclone genesis from remotely sensed infrared image data. *IEEE Geosci. Remote Sens. Lett.* **7**, 826–830 (2010).
29. O. G. Rodríguez-Herrera, K. M. Wood, K. P. Dolling, W. T. Black, E. A. Ritchie, J. S. Tyo, Automatic tracking of pregenesis tropical disturbances within the deviation angle variance system. *IEEE Geoscience and Remote Sensing Letters.* **12**, 254–258 (2014).
30. C. Zhang, X. Wang, C. Duanmu, Tropical cyclone cloud image segmentation by the B-spline histogram with multi-scale transforms. *Acta Meteorologica Sinica.* **24**, 78–94 (2010).
31. J. A. Knaff, C. J. Slocum, K. D. Musgrave, C. R. Sampson, B. R. Strahl, Using routinely available information to estimate tropical cyclone wind structure. *Monthly Weather Review.* **144**, 1233–1247 (2016).
32. K. Dolling, E. A. Ritchie, J. S. Tyo, The use of the deviation angle variance technique on geostationary satellite imagery to estimate tropical cyclone size parameters. *Wea. Forecasting.* **31**, 1625–1642 (2016).
33. C. Kummerow, W. Barnes, T. Kozu, J. Shiue, J. Simpson, The tropical rainfall measuring mission (TRMM) sensor package. *Journal of atmospheric and oceanic technology*, **15**, 809–817. (1998).
34. A. Y. Hou, R. K. Kakar, S. Neeck, A. A. Azarbarzin, C. D. Kummerow, M. Kojima, O. Riko N. Kenji, T. Iguchi, The global precipitation measurement mission. *Bulletin of the American Meteorological Society.* **95**, 701–722 (2014).
35. O. Guzman, H. Jiang. Global increase in tropical cyclone rain rate. *Nature communications.* **12**, 1–8 (2021).
36. T. Fiolleau, R. Roca, An algorithm for the detection and tracking of tropical mesoscale convective systems using infrared images from geostationary satellite. *IEEE transactions on Geoscience and Remote Sensing*, **51**, 4302–4315 (2013).
37. K. T. Nguyen, L. Hu, A. S. Alenin, E. A. Ritchie, J. S. Tyo, A Satellite-Based Remote-Sensing Framework to Quantify the Upwelling Radiation Due to Tropical Cyclones. *IEEE Journal of Selected Topics in Applied Earth Observations and Remote Sensing*, **14**, 5488–5500 (2021).
38. T. S. L'Ecuyer, "Earth's energy balance" in *International Encyclopedia of Geography: People, the Earth, Environment and Technology*. (John Wiley & Sons, Ltd. Lee, K. 2017).
39. B. C. Trabling, M. M. Bell, B. R. Brown, Impacts of radiation and upper-tropospheric temperatures on tropical cyclone structure and intensity. *Journal of the Atmospheric Sciences.* **76**, 135–153 (2019).

40. H. R. James, A. A. Wing, X. Tang, Erika. L. Duran. The critical role of cloud–infrared radiation feedback in tropical cyclone development. *PNAS*, 117 (45), 27884–27892. (2020).
41. A. Maggiorano. Impacts of extreme events on the ocean thermal structure over the North West Shelf of Australia: Part 1. The hydrodynamic drivers of the 2012/2013 marine heatwave; and Part 2. Effects of tropical cyclones on the ocean thermal balance. *PhD thesis, University of New South Wales*. <https://doi.org/10.26190/unsworks/1989> (2022).
42. T. Knutson, S. J. Camargo, J. C. Chan, K. Emanuel, C. H. Ho, J. Kossin, M. Mohapatra, M. Satoh, M. Sugi, K. Walsh, L. Wu, Tropical cyclones and climate change assessment: Part II: Projected response to anthropogenic warming. *Bulletin of the American Meteorological Society*. **101**, E303-E322 (2020).
43. J. P. Kossin, K. R. Knapp, T. L. Olander, C. S. Velden, Global increase in major tropical cyclone exceedance probability over the past four decades. *Proc. Nat. Acad. Sci. United States Amer.* **117**, 11975–11980 (2020).
44. K. Knapp, S. Applequist, H. Diamond, J. Kossin, M. Kruk, C. Schreck, “NCDC International Best Track Archive for Climate Stewardship (IBTrACS) Project, Version 3” (2010).
45. J. Janowiak, B. Joyce, P. Xie. “NCEP/CPC L3 Half Hourly 4km Global (60S – 60N) Merged IR V1”, (Greenbelt, MD, Goddard Earth Sciences Data and Information Services Center, 2017).
46. Doelling, D. “CERES Level 3 SYN1deg-1Hour Terra-Aqua-MODIS HDF4 file–Edition 4A, Data set”, (NASA Langley Atmospheric Science Data Center DAAC, 2017).

Figures

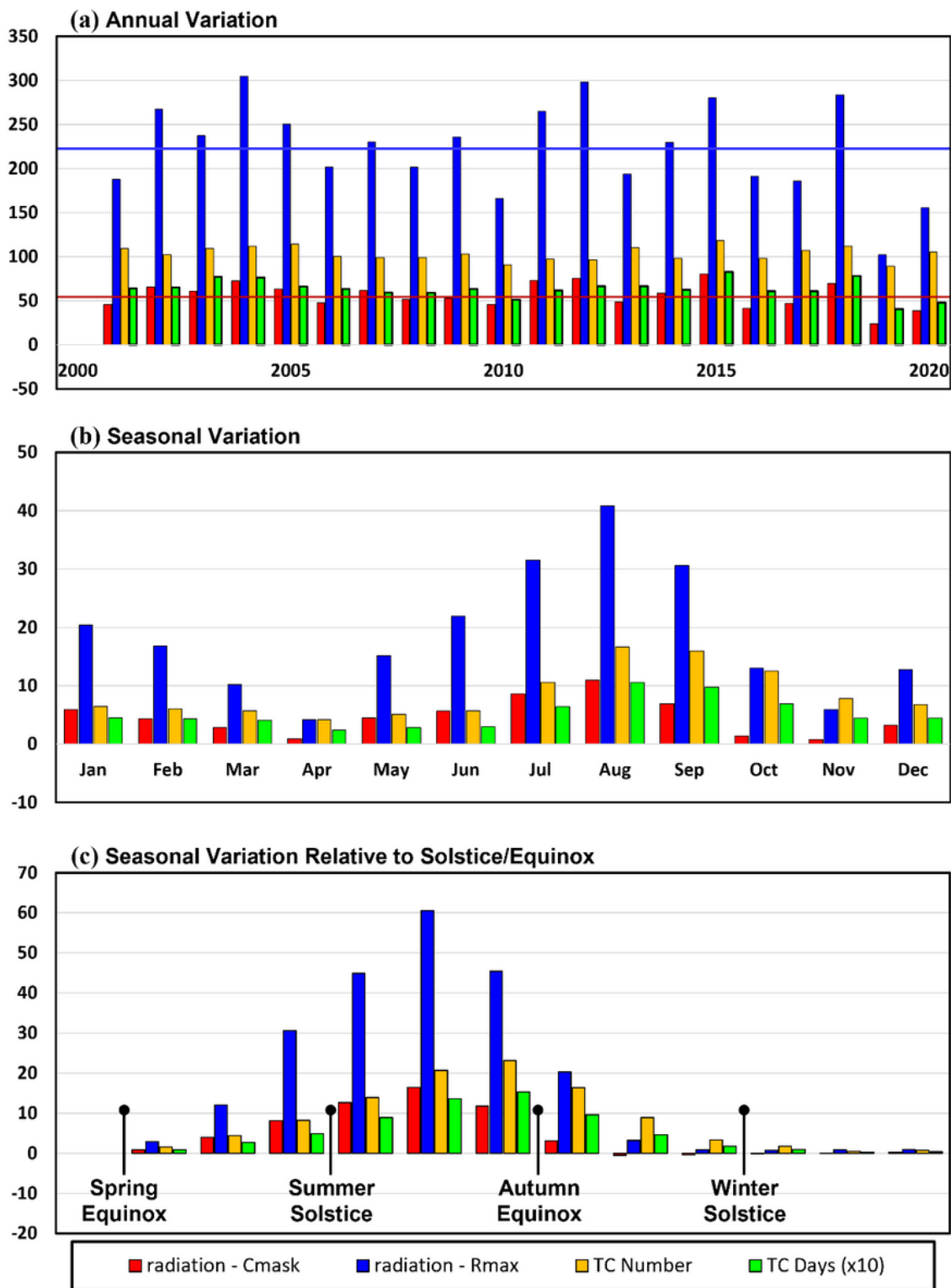
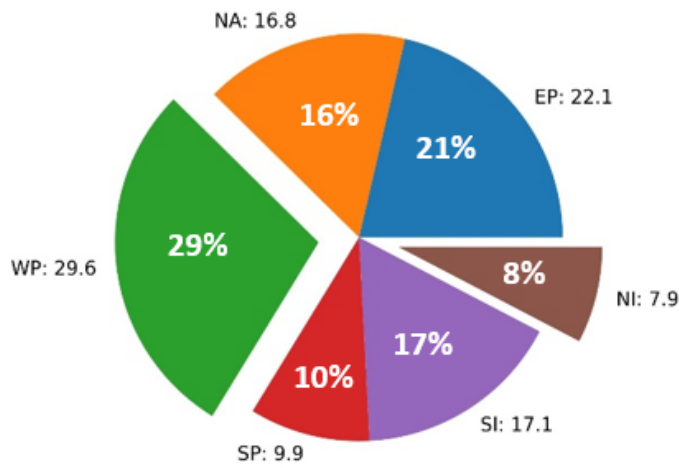


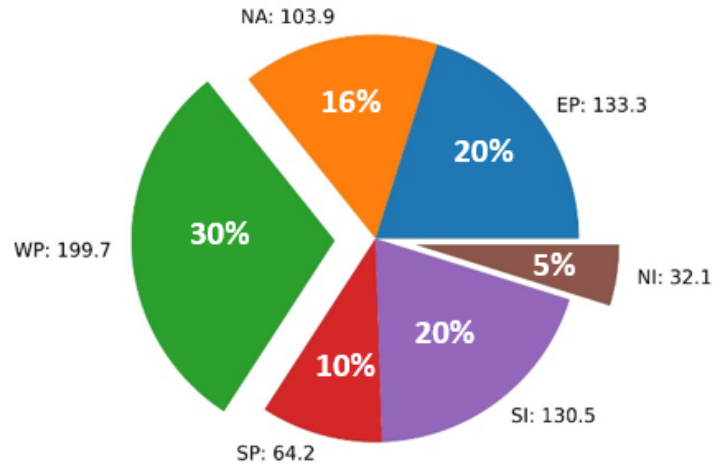
Figure 1

(a) Annual and (b) seasonal variation of tropical cyclone net radiation (TW) calculated using the C_{mask} (red) and R_{max} (blue), number of tropical cyclones (orange), and the number of tropical cyclone days (x 10) (green). The red and blue lines indicate the average annual tropical cyclone net radiation for the C_{mask} (red) and R_{max} (blue) calculations, respectively.

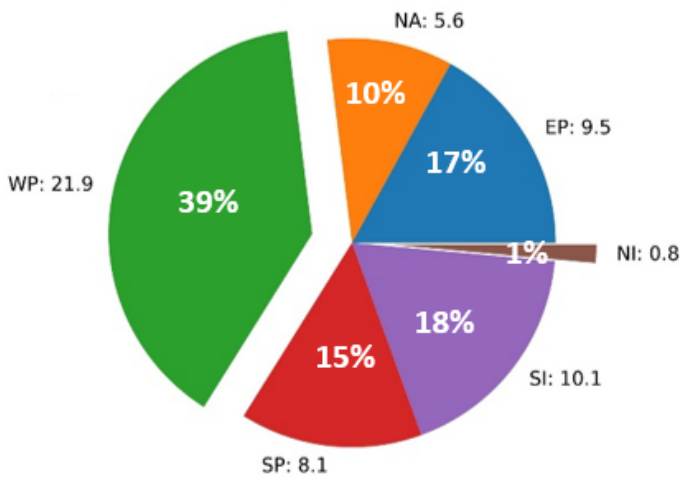
(a) Tropical Cyclone Number



(b) Tropical Cyclone Days



(c) Net tropical cyclone radiation - C_{mask}



(d) Net tropical cyclone radiation - R_{max}

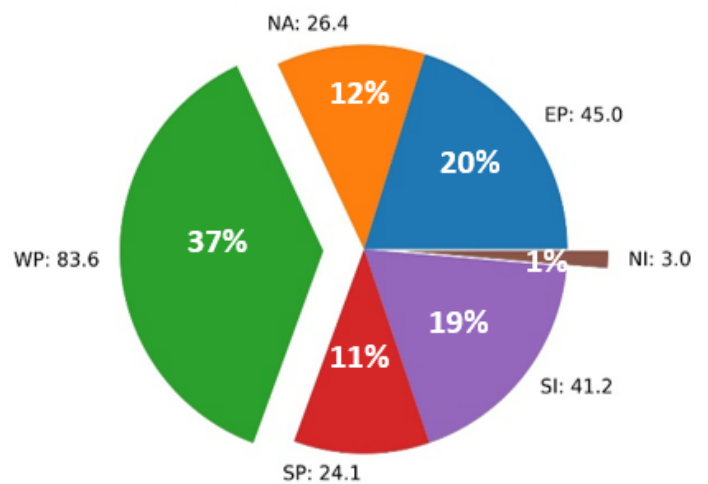


Figure 2

Annual average: (a) tropical cyclone number; (b) number of tropical cyclone days; (c) tropical cyclone net radiation (Units: TW) using the C_{mask} calculation; and (d) same as (c) but using the R_{max} calculation for all six basins.

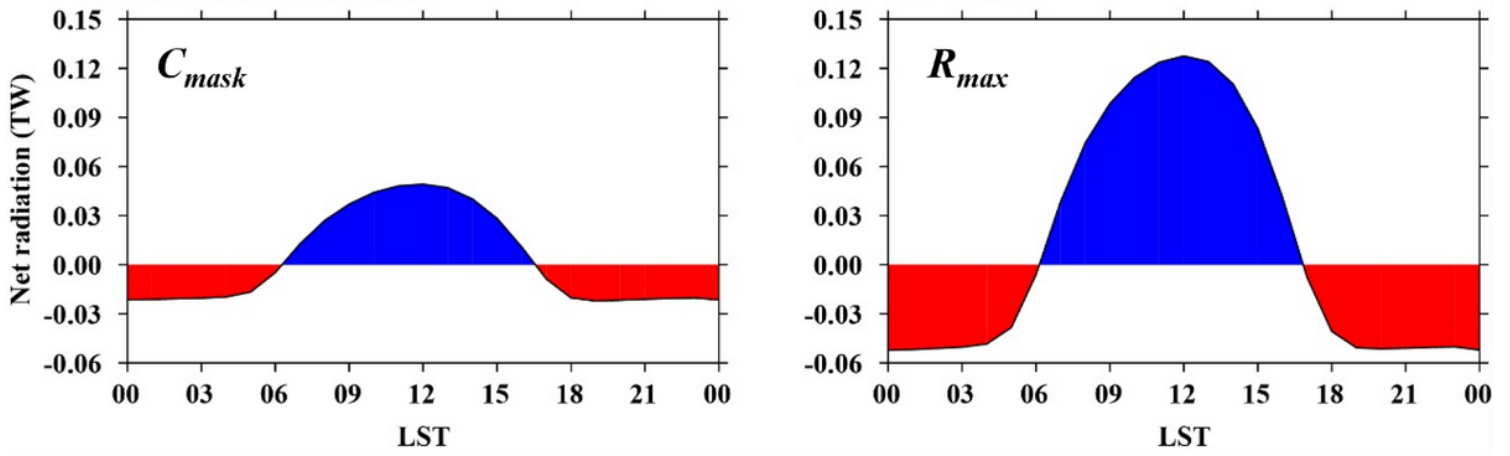


Figure 3

The average daily diurnal cycle of net radiation per tropical cyclone over the 20-year period (TW): (a) the C_{mask} ; and (B) the R_{max} calculation. Blue shading indicates positive net radiation (cooling) and red shading indicates negative net radiation (warming).

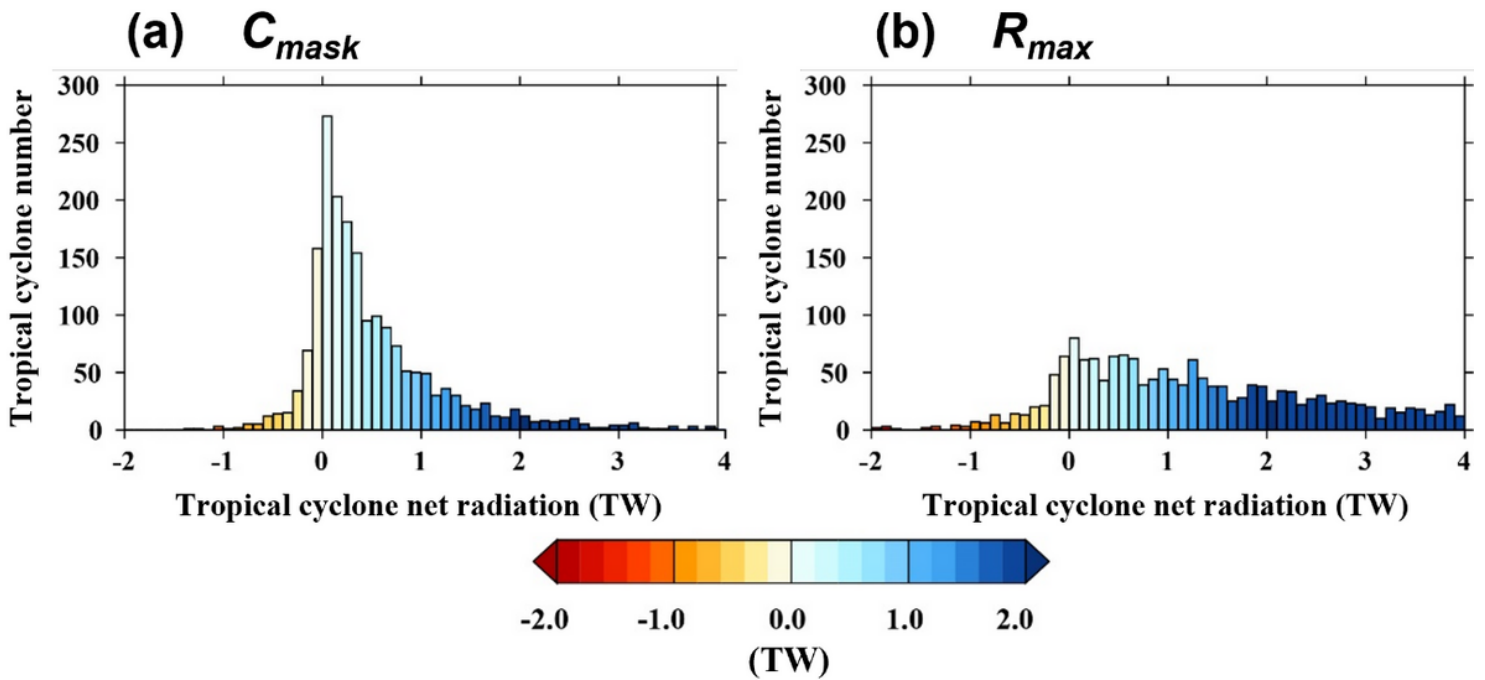


Figure 4

Frequency distribution of tropical cyclone net radiation calculated over the lifetime of each tropical cyclone for the period 2001-2020 using the: (a) C_{mask} ; and (b) R_{max} calculation.

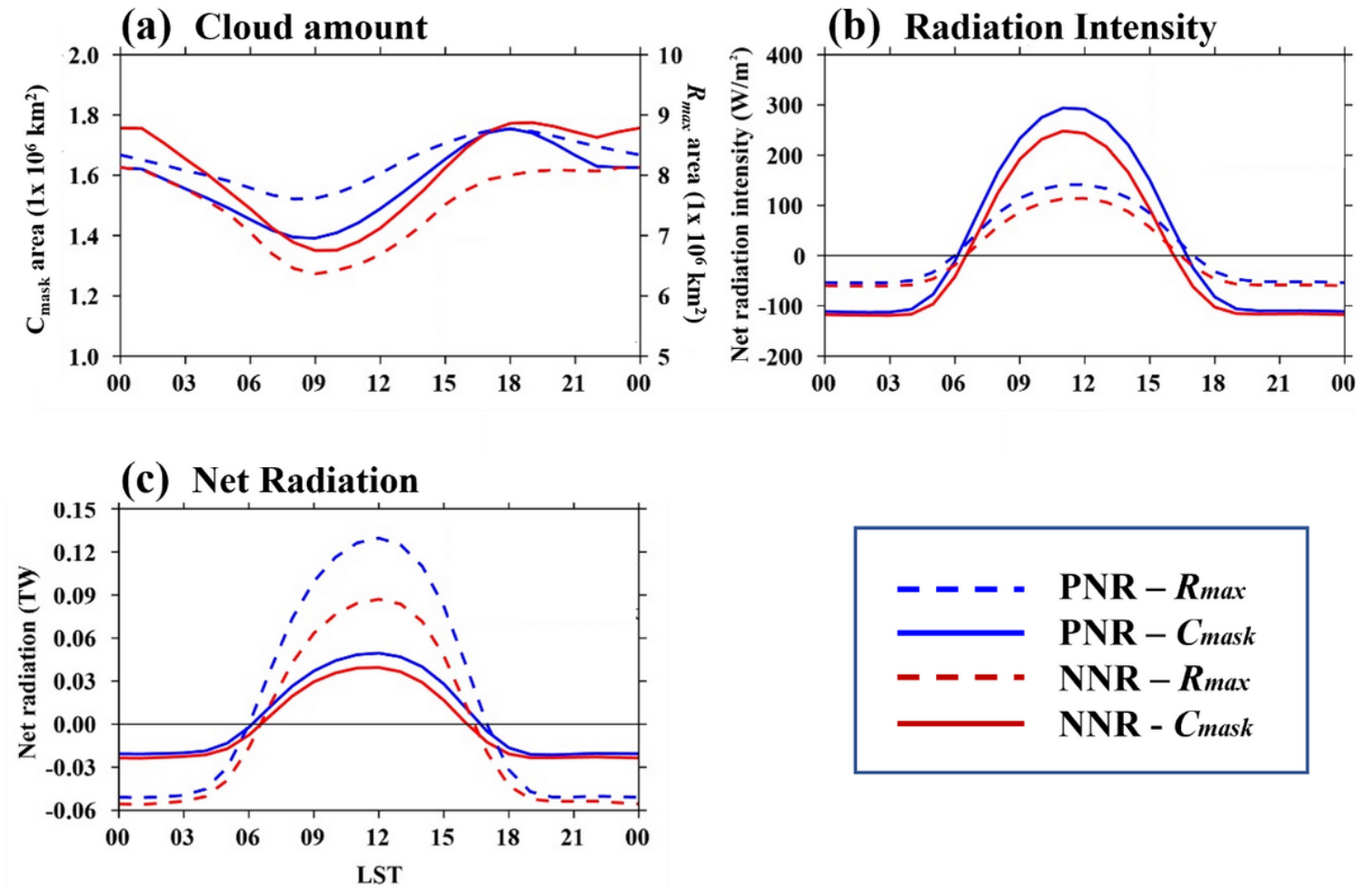


Figure 5

The average daily diurnal cycle of net radiation per tropical cyclone over the 20-year period (TW) separated out by PNR (blue) and NNR (red) tropical cyclones for: (a) the tropical cyclone cloud area; (b) tropical cyclone net radiation intensity; and (c) tropical cyclone net radiation for the C_{mask} (solid) and R_{max} (dashed) calculation.

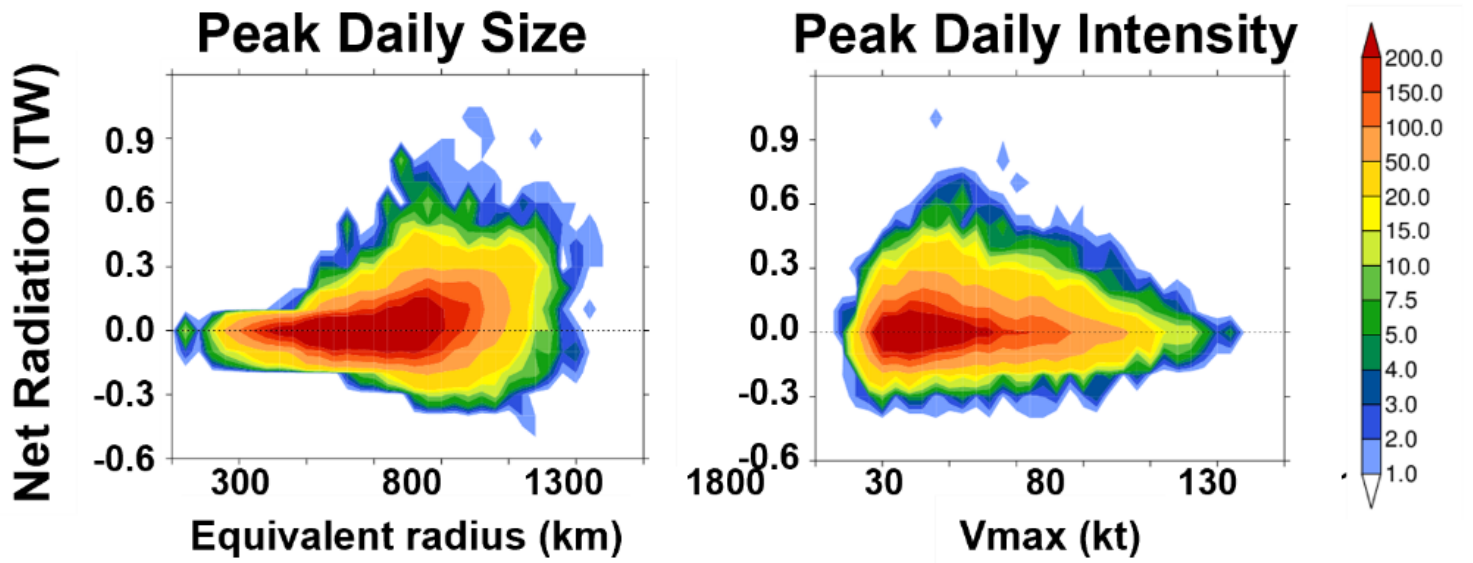


Figure 6

Frequency distribution of daily global tropical cyclone net radiation using the C_{mask} sorted by daily peak size and daily peak intensity. Size is calculated as the equivalent radius of a circle with the same number of pixels as the cloud mask.

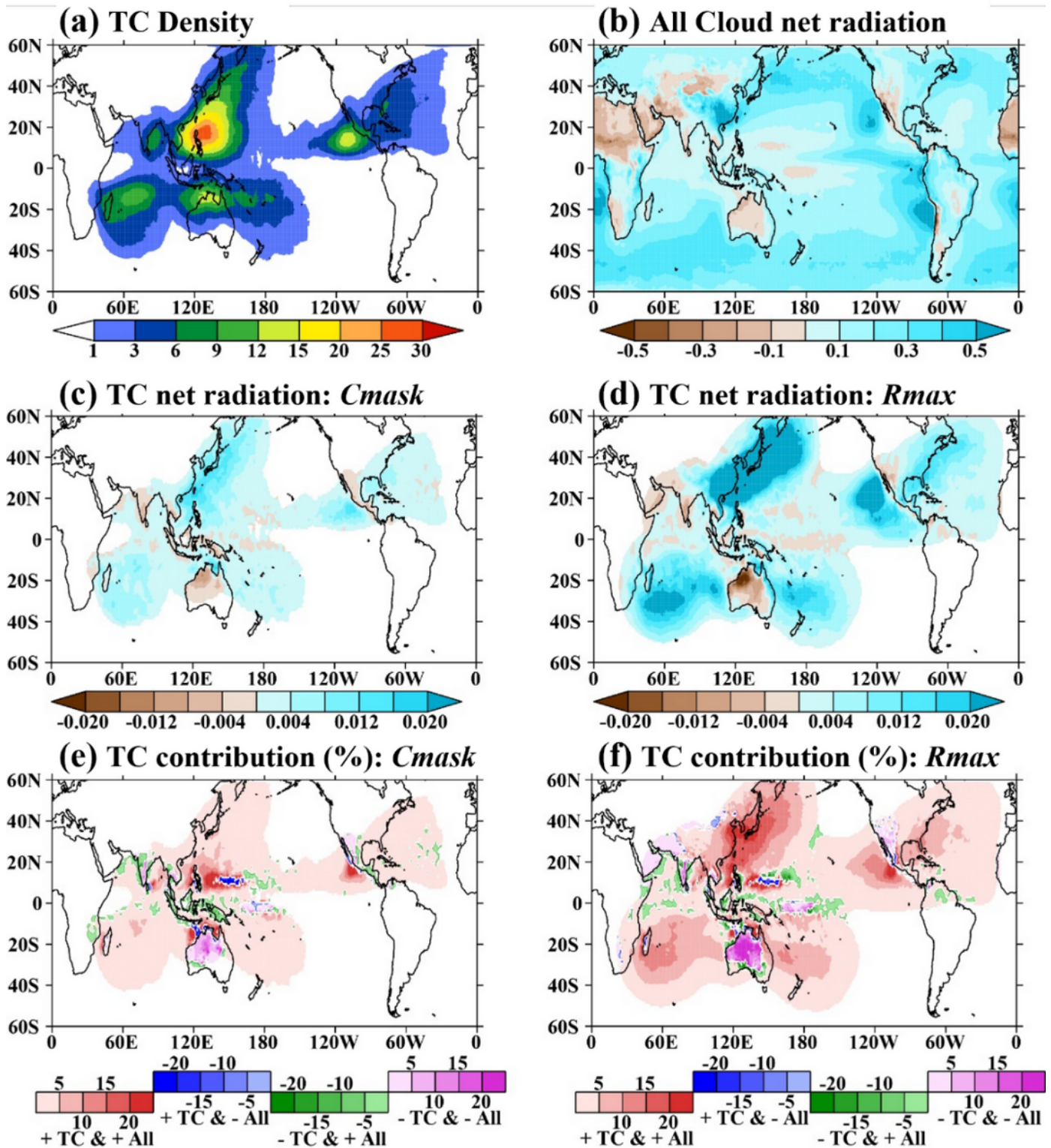


Figure 7

The spatial distribution of: (a) tropical cyclone cloud frequency density (days); (b) all cloud net radiation (TW); (c) tropical cyclone net radiation (TW); and (e) the contribution to all cloud net radiation from the annual average during 2001-2020 (%); (d) and (f) same as (c) and (e) except calculated using R_{max} . In (e) and (f), the red shading indicates regions where both the tropical cyclone and all cloud net radiation is positive (cooling), blue shading is positive tropical cyclone (cooling) and negative all cloud (warming) net

radiation, green shading is negative tropical cyclone (warming) and positive all cloud (cooling) net radiation, and pink is both tropical cyclone and all clouds negative net radiation. The negative percentage indicates that the sign of the net radiation due to tropical cyclones is opposite that of the “all cloud” net radiation.

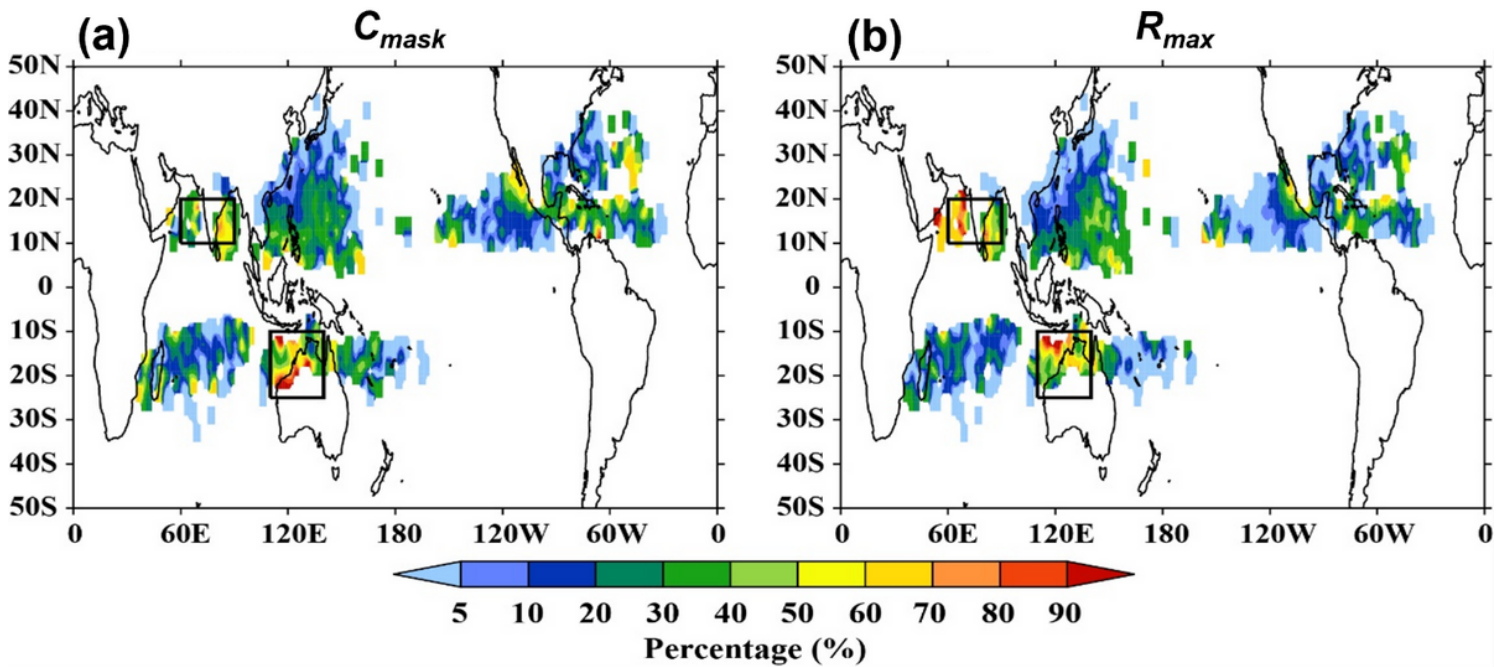


Figure 8

The spatial distribution of NNR tropical cyclones by 24-hour period as a percentage of total using the: (a) C_{mask} ; and (b) R_{max} calculation. The grid box resolution is 1 degree by 1 degree.

Supplementary Files

This is a list of supplementary files associated with this preprint. Click to download.

- [HRT2022NatureCSupplementaryMaterial.pdf](#)